New technique for computation and challenges for electron-beam lithography

Xiaokang Huang, Greg Bazán, and Gary H. Bernstein
Department of Electrical Engineering, University of Notre Dame, Notre Dame, Indiana 46556

(Received 15 June 1993; accepted 20 August 1993)

In this article, the basic concepts of our recently proposed computing architecture based on Coulomb coupling of nanofabricated structures, called quantum cellular automata (QCA) are reviewed and fabrication issues critical to the new technology are discussed. The QCA fabrication will require an extremely high level of lithographic control. To this end, the proximity effects in making very high density patterns with poly(methylmethacrylate) (PMMA) and electron-beam lithography have been experimentally investigated. A triple Gaussian model was used to simulate the experimental data. By using a 50 keV electron beam, sub-40 nm pitch gratings, double lines, and dot grids were successfully fabricated on Si and SiO_2/Si bulk wafers with single-level PMMA and lift-off.

I. INTRODUCTION

High density patterns are very important for such structures as quantum devices and high speed photodetectors,[1] as well as studies of basic quantum phenomena, such as current drag.[2] Recently, we proposed a new paradigm for computing with cellular automata (CA) composed of arrays of quantum dots arranged into separate cells of several dots.[3,4] We call this new architecture "quantum cellular automata" (QCA). Our calculations show that the dots, which are fundamental to the new architecture (discussed below), must be as small as 10–15 nm in diameter on a pitch of 15–30 nm with intracell variations of at most 5%–10% over a few micron area. This implies that electron-beam lithography (EBL) to be used in the fabrication will be put to a serious test. Although Allee *et al.*[5,6] have directly patterned 15 nm gratings on SiO_2/Si with EB irradiation, lift-off with poly(methylmethacrylate) (PMMA) is still one of the most common techniques used in pattern transfer. The latter has so far produced results in the 40–50 nm pitch range.[1] In this size regime, pitch is limited by the strength of PMMA and proximity effects during exposure.

Proximity effects result from the distributions of injected and scattered electrons in the resist. Because of the distributions, the resist which is not directly addressed by the primary EB will also be exposed. The electron distributions in resist have been discussed in many papers,[7–9] and a triple Gaussian model[8–10] was used in modeling the distributions. The triple Gaussian model is

$$f(r)=\frac{1}{\pi(1+\eta+\eta')}\left[\frac{1}{\alpha^2}\exp\left(-\frac{r^2}{\alpha^2}\right)+\frac{\eta}{\beta^2}\exp\left(-\frac{r^2}{\beta^2}\right)+\frac{\eta'}{\gamma^2}\exp\left(-\frac{r^2}{\gamma^2}\right)\right]. \quad (1)$$

The first term includes the distributions of the primary electron beam and forward scattered electrons. The width of the term α ranges from a few nm to tens of nm, which depends on the beam size and energy, and the resist. The second term only includes the backscattered electrons from the substrate. The width of the distribution of backscattered electrons β is a few microns and depends on beam energies and types of substrates. The higher the beam energy, the wider the distribution.[11] The third term, the "broad range electrons,"[10] describes the behavior of all other electrons that are not included in the first two terms.[8,9] Its width γ is a few hundreds of nm. Here, η and η' are the ratios of the exposures of the β and γ term to the forward exposure, respectively.

Because of their distributions, different electrons result in proximity effects in different ranges. Although there are many papers that have investigated the proximity effects in EBL[8,9,12] and many methods for computer-aided proximity effect corrections during EBL have been developed,[13,14] the feature sizes and spacing in most of the published work are in the half- or quarter-micron regime, which is important in ultra-large scale integration (ULSI) circuit fabrication. Since large throughput is required in manufacturing, low beam energy (20 keV) and large currents are used in industrial EBL. In that case, backscattered electrons can dominate the proximity effects. However, for making very high density patterns that approach the spatial density limit of EBL, high beam energy (50 keV or higher), and small beam size (smaller than 10 nm) are usually used. In applications of nanolithography for quantum devices, pattern sizes are usually very small compared to those of ULSI. Therefore, the proximity effects from forward scattered electrons and secondary electrons become more pronounced.[10]

In this article, we discuss the basic properties and requirements of the QCA architecture. Toward the achievement of the required size scales, we report an experimental investigation of proximity effects for lines with pitch down to 50 nm. A triple Gaussian model is used in the theoretical simulation of the experimental results. The purpose of discussing the proximity effects is not directly to make proximity corrections in processing, but to understand and overcome the difficulties in making high density patterns. A spatial density limit in gratings caused by the proximity effects in PMMA is also determined. We studied the proximity effects in gratings rather than in arrays of dots (which will be more typical of the QCA work to be done)

 ©1993 American Vacuum Society

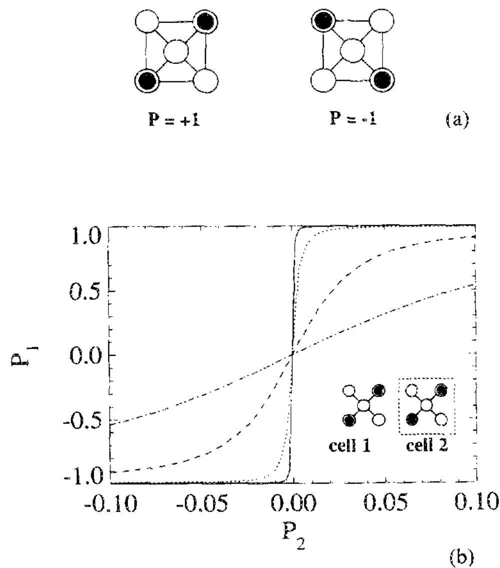

FIG. 1. (a) The quantum cell consisting of five quantum dots which are occupied by two electrons. The mutual Coulombic repulsion between the electrons results in bistability between the $P=+1$ and $P=-1$ states. (b) The cell–cell response function for various values of the dot-to-dot coupling energy t. The induced cell polarization P_1 is plotted as a function of the neighboring cell polarization P_2. The results are shown for values of $t=-0.2$ (full curve), -0.3 (dotted curve), -0.5 (dashed curve), and -0.7 (dot–dashed curve) meV. Note that the response is shown only for P_2 in the range $[-0.1,+0.1]$.

since gratings are more susceptible to proximity effects due to larger integration of dose, and the results would be more easily interpretable. The results discussed below can be applied to structures which require spacing in the sub-50 nm range. Toward this goal, 38 nm pitch gratings, 36 nm pitch double lines, and 37 nm pitch dot grid on Si and SiO_2/Si bulk substrates were successfully made with 50 keV EBL combined with the lift-off technique.

II. QUANTUM CELLULAR AUTOMATA (QCA)

QCA consist of separate cells containing several quantum dots per cell, as shown in Fig. 1(a). We have proposed a specific realization of these ideas using two-electron cells composed of quantum dots, which we will later show is within the reach of current fabrication technology. We define polarization as an average of the two-electron wave function as defined in Refs. 3 and 4. If the charge is aligned along one axis as shown in Fig. 1(a), the polarization is "+1" (encoding the binary value "1") and when distributed along the other axis the polarization is "−1" (encoding the binary value "0"). The mutual Coulomb repulsion of the two electrons causes the charge density in the cell to be very highly polarized (aligned) along one of the two cell axes, suggestive of a two-state CA. Figure 1(b) shows the polarization of a two-electron cell due to the polarization of an adjoining cell for various values of the dot-to-dot coupling energy, t (which depends on the intracell barrier heights and intracell dot spacing). The polarization of one cell induces a polarization in a neighboring cell through the Coulomb interaction in a very nonlinear fashion.

Electrons within the cells are coupled quantum mechanically by tunneling between sites, but coupling between cells is strictly by Coulomb interactions. The cells are arranged in arrays which interact to perform computational functions. Computing in the new paradigm is edge driven. Input, output, and power are delivered to the edge of the array only; no direct flow of information or energy to internal cells is required. The architecture is so designed that the ground state configuration of the array, subject to boundary conditions determined by the inputs, yields the computational result. We refer to computations performed in this manner as "computing in the ground state."

Device modeling has been performed by solving the two-electron Schrödinger equation directly for each cell. Arrays of cells were modeled using a self-consistent Hartree technique based on the two-electron problem in each cell. We have shown[3,4] that useful computing structures can be built from a set of logical primitives composed of quantum cells. This set includes wires, wire crossings, inverters, and a flexible three-input structure. The three-input device can be configured as an AND gate, an OR gate, or a majority logic unit. The reader is referred to the references for a complete description of these logic devices.

The precise nature of the cell fabrication is critical to the success of the CA. The QCA cell arrays are forgiving of variations of dot size and spacing when variations occur only between adjoining cells, but not within a cell. Figure 1(b) shows that the resulting polarization of a cell is very large when subjected to only a small polarization of the input cell. This implies that spacing between cells is not very critical since the Coulomb interactions affected by variations in distance are equivalent to variations of polarization. However, if a cell contains dots of various sizes, then it is prebiased toward one or the other state. Although this can be very useful in some cases,[3,4] if uncontrolled, the state of the cell would be very difficult to control accurately. The remainder of this article is devoted to an experimental investigation of the role of proximity effects in obtaining very dense patterns such as those likely to be used in QCA fabrication.

III. EXPERIMENTAL PROCEDURE

Single layers of 950K PMMA 50–70 nm thick were spun on bulk Si and SiO_2/Si substrates. The thickness of the SiO_2 in all cases was 200 nm. Patterns were written at 50 keV with an Amray 1400 scanning electron microscope employing a W cathode, customized as an EBL system.[15] After exposure, samples were developed with methylisobutylketone:isopropanol:methylethylketone (MIBK:IPA:MEK) (1:3:0.06) maintained at 26 °C. At this temperature, the contrast of the developer has been demonstrated to be larger than 10.[16] Our samples were not rinsed with pure methanol, as is typically done following development.[1] We have found[17] that methanol and other solutions weaken the strength of PMMA walls and limit the space between patterns, and that in fact this rinse step is not necessary. We found that replacing this step by drying in pure N_2 immediately after development is of benefit to the strength of the PMMA walls, and therefore helps to

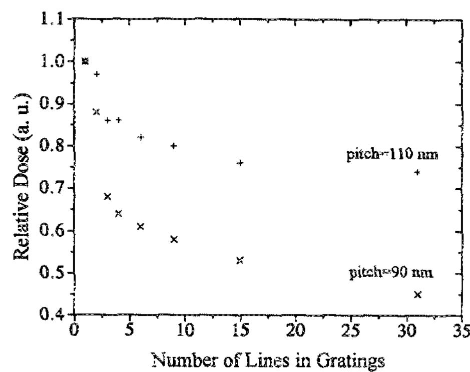

FIG. 2. Experimental results of the relative dose as a function of number of lines in gratings. +:110 nm pitch gratings; ×:90 nm pitch gratings.

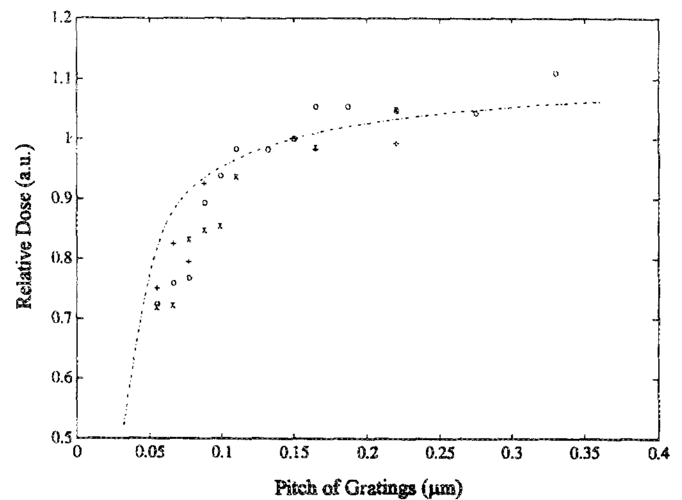

FIG. 3. The relation between the relative dose and the pitch of gratings. ○, ×, and + are separate sets of experimental results. The dot–dashed line is the simulation with the triple Gaussian model.

achieve high density patterns with lift-off. Au or Ti/Au was evaporated with an EB evaporator followed by lift-off with acetone soaking and shooting with a syringe.[18]

The relationship between resulting linewidth w and (single-pass) line dose $D_{\rm line}$ (defined in units of C/cm) is approximately linear at lower doses and saturates at higher doses,[18,19] yielding a relationship for the average area dose $D_{\rm area}$ in the linear region as,

$$D_{\rm area}=D_{\rm line}/w({\rm C/cm^2}). \quad (2)$$

This implies that in all of our exposures at low doses and narrow lines, the average dose across the developed area of the line is constant regardless of the final linewidth.

IV. RESULTS AND DISCUSSION

As discussed above, the linewidth increases linearly with small exposure doses. If two lines are exposed near each other, each line will get extra exposure dose from the other line exposure because of proximity effects. In order to achieve the same linewidth, the average area dose defined by Eq. (2) should be smaller in two close lines than in a single line pattern. This means that the slopes in the relation between linewidth and exposure dose will be different in the two cases.[18] We define relative dose as the ratio of the average area dose of multiline patterns to the average area dose of a single line pattern. Figure 2 shows the relative dose as a function of the number of lines in a pattern. As expected, relative dose decreases as more lines are added into the pattern because of interline exposure by the proximity effects. Also the relative dose decreases when lines get closer together. This can be seen more clearly in Fig. 3 which shows the relative dose as a function of the line pitch of gratings. The gratings in our study were 3 μm×3 μm separated by 2 μm spaces. Linewidths were measured at the center of gratings and ranged from 20 to 45 nm for different pitch gratings. This is different from ULSI in which equal space and linewidth are important,[9] since this is not typically necessary for quantum device applications. In Fig. 3, the relative dose was defined as the ratio of the average area doses of gratings to those of the 150 nm pitch gratings. The dot–dashed line in Fig. 3 is a calculated result using Eq. (1).[20] In our calculation, we use $\beta=10$ μm and $\eta=0.8$ for 50 keV backscattered electrons in solid silicon substrates according to Ref. 11. Ideally, α should be determined by a convolution of the beam shape with the lateral scattering profile within the resist.[21] Since this is complicated by knowledge of the exact shape of the beam and lateral scattering properties, we instead fit the experimental data.[8,9,12] For the best fit, α, γ, and η' were chosen as $\alpha=0.029$ μm, $\gamma=0.4$ μm, and $\eta'=0.35$. Although backscattered electrons from other gratings also contributed to the total dose, it is appropriate to neglect them in our case since $\eta/\beta^2 \ll 1/\alpha$ and η'/γ^2, and the total area of all other gratings within a range of β away from the center was small. From Fig. 3, it can be seen that the relative dose decreases very quickly for line pitch smaller than 100 nm, while it is relatively flat for line pitch larger than 150 nm. Relative dose as a function of pitch of double lines also shows a similar relation.[19]

The different relationship between the relative dose and the pitch of gratings is due to the proximity effects from primary, forward, backscattered, and long-range electron distributions. This has been presented in Ref. 10. Figure 3 is important because it not only shows the significant proximity effects caused by forward scattered electrons and fast secondary electrons, but it is also very useful in predicting the dose needed to achieve certain pitch gratings with required linewidth in EBL.

By using Eq. (1), the minimum exposure received between lines (E_v) and the maximum exposure received by the lines (E_p) can be calculated. The larger the ratio E_v/E_P, the more difficult the task faced by the developer and the higher must be the contrast of the developer utilized in order to delineate the latent image. Figure 4 shows E_v/E_P as a function of the grating pitch. β, γ, η, and η' were the same as in the calculation in Fig. 3, while different widths of forward scattered electrons (α) were used in the calculation. The shift of the E_v/E_P curve to the left as α decreases means that higher spatial density can be achieved for smaller α. Also E_v/E_p changes with grating pitch and

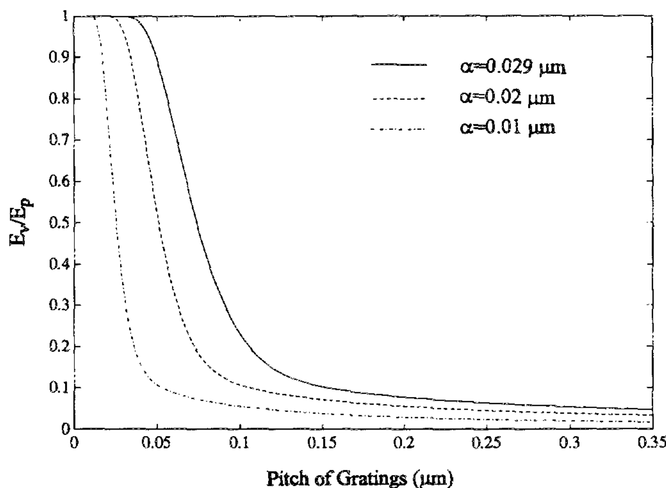

FIG. 4. E_v/E_P as a function of the pitch of gratings. E_v is the minimum exposure received between lines, and E_P is the maximum exposure received on the lines.

approaches unity when lines are very close. In that case, patterns are washed out. The role of the developer is to distinguish E_v and E_P to produce the required patterns. For a given developer contrast, there is a maximum E_v/E_P that can still be distinguished by the developer. E_v/E_P can be related to D_i/D_f, where D_i is the exposure dose at the onset of development and D_f is the exposure dose for complete development, and developer contrast γ^* is defined as $1/\log(D_i/D_f)$. Therefore, the minimum pitch that can be achieved with the developer can be obtained from Fig. 4. We used a very high contrast developer in our experiments. The contrast for our developer is greater than 10 at 26 °C,[16] so it can distinguish E_P from E_v at $E_v/E_P \sim 0.8$ or even higher. Therefore, only 50–60 nm pitch gratings could be expected in our proximity effect experiments in which 4 pA beam current was used. However, with $\alpha = 10$ nm,[7] 20 nm pitch gratings can be expected.

Guided by the discussion above, the beam current was decreased from 4 to 2.5 pA. Although this made focusing more difficult because of image noise, by carefully focusing of a narrower beam, we achieved a minimum grating pitch of 38 nm, as shown in Fig. 5(a). In order to get this result, Fig. 3 was used with Eq. (2) to determine the best line dose range needed in the exposure. Also, extreme care was taken during the development because any overdevelopment could cause the lines to wash out. These data points are not shown in Fig. 3 for two reasons. First, α was changed as the beam current decreased. Second, the linewidth of the 38 nm pitch grating could not be accurately measured because of the resolution of our scanning electron micrograph (SEM), so it was difficult to get the accurate area dose required in Fig. 3. The grating is made by Ti/Au (2 nm/15 nm) on top of SiO_2/Si by lift-off. 36 nm pitch double lines made by lift-off are shown in Fig. 5(b). Since there is less proximity effect in double lines than in gratings, as shown in Fig. 2, making dense double lines is easier than making dense gratings. However, besides proximity effects, the spatial density of EBL is also limited by

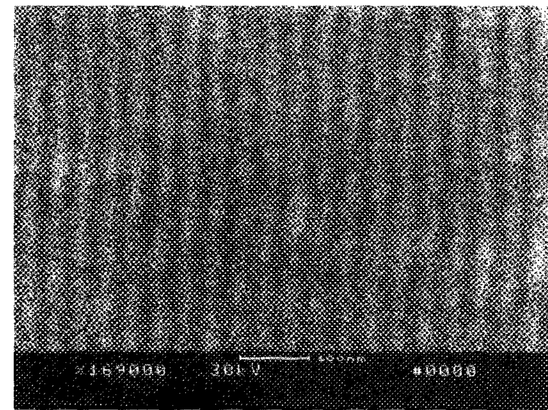

(a)

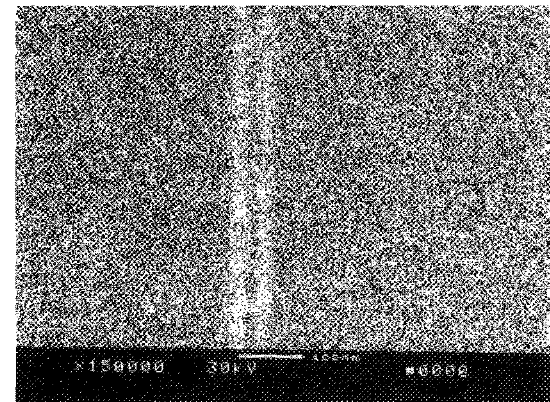

(b)

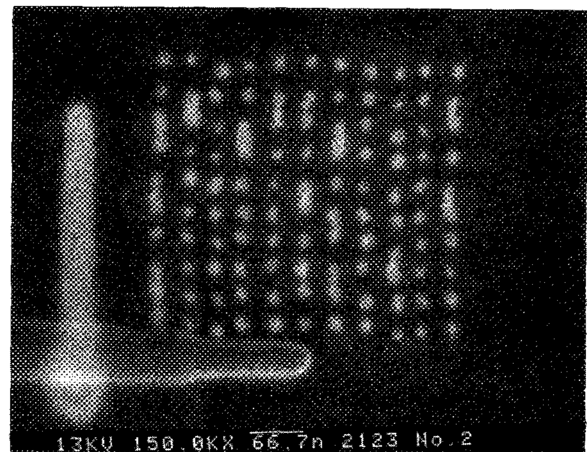

(c)

FIG. 5. (a) A Ti/Au (2 nm/15 nm) grating with 38 nm pitch; (b) A lift-off Ti/Au (2 nm/15 nm) double lines with 36 nm center-to-center distance; both (a) and (b) are made by lift-off on SiO_2/Si substrates. (c) A gold (15 nm thick) dot grid on Si substrate with 37 nm pitch by lift-off.

the minimum fundamentally achievable linewidth and space. The former (linewidth) is determined by beam size and fast secondary electrons (intraline proximity effect), and is ~10 nm.[7] The latter (space) is dominated by the strength of PMMA,[17,22] and is also ~10 nm for 45 nm thick resist. This means that the minimum achievable pitch of double lines is ~20 nm, i.e., the same as the minimum expected pitch of gratings limited by all proximity effects. A 37 nm pitch dot grid is shown in Fig. 5(c). It is 15 nm

thick Au on a Si substrate made by lift-off. This micrograph was obtained with a Topcon model ABT-150F field emission SEM. Since there is much less proximity effect in making dot grids, and the strength of PMMA is not as important in this case, 10 nm diam dots with 15 nm pitch dot grids can be expected.

V. SUMMARY AND CONCLUSIONS

We discussed a new paradigm in computing called quantum cellular automata and related the physical properties of the quantum structures to the limits of EBL. We investigated proximity effects in order to predict the ultimate size of the achievable dot arrays for QCA applications. We investigated properties of dense gratings and dot arrays with a minimum achieved double line pitch of 36 nm. We predict that dot arrays with a pitch of 15 nm should be achievable. Thus, the requirements for the fabrication of dense arrays of dots for applications to quantum cellular automata are predicted to be within the physical limits of lift-off technology using PMMA resist and EBL.

ACKNOWLEDGMENTS

The authors thank W. Porod, C. S. Lent, and P. D. Tougaw for helpful discussions. This work was supported by the National Science Foundation, the National Space Grant College and Fellowship Program, the Air Force Office of Scientific Research, and the Office of Naval Research. They also thank Topcon Technologies Inc. for providing field emission SEM micrographs.

[1] P. B. Fischer and S. Y. Chou, Appl. Phys. Lett. **62**, 2989 (1993).
[2] A. G. Rojo and G. D. Mahan, Phys. Rev. Lett. **68**, 2074 (1992).
[3] C. S. Lent, P. D. Tougaw, and W. Porod, Appl. Phys. Lett. **62**, 714 (1993).
[4] C. S. Leng, P. D. Tougaw, W. Porod, and G. H. Bernstein, Nanotechnology **4**, 49 (1993).
[5] D. R. Allee and A. N. Broers, Appl. Phys. Lett. **57**, 2271 (1990).
[6] D. R. Allee, C. P. Umbach, and A. N. Broers, J. Vac. Sci. Technol. B **9**, 2838 (1991).
[7] D. C. Joy, Microelectron. Eng. **1**, 103 (1983).
[8] R. J. Bojko and B. J. Hughes, J. Vac. Sci. Technol. B **8**, 1909 (1990).
[9] S. J. Wind, M. G. Rosenfield, G. Pepper, W. W. Molzen, and P. D. Gerber, J. Vac. Sci. Technol. B **7**, 1507 (1989); M. G. Rosenfield, S. J. Wind, W. W. Molzen, and P. D. Gerber, Microelectron. Eng. **11**, 617 (1990).
[10] X. Huang, G. H. Bernstein, G. Bazán, and D. A. Hill, J. Vac. Sci. Technol. A **11**, 1739 (1993).
[11] P. M. Mankiewich, L. D. Jackel, and R. E. Howard, J. Vac. Sci. Technol. B **3**, 174 (1985).
[12] S. A. Rishton and D. P. Kern, J. Vac. Sci. Technol. B **5**, 135 (1987).
[13] R. C. Frye, J. Vac. Sci. Technol. B **9**, 3054 (1991).
[14] S. Y. Lee, J. C. Jacob, C. M. Chen, J. A. McMillan, and N. C. McDonald, J. Vac. Sci. Technol. B **9**, 3048 (1991).
[15] G. Bazán and G. H. Bernstein, J. Vac. Sci. Technol. A **11**, 1745 (1993).
[16] G. H. Bernstein, D. A. Hill, and W.-P. Liu, J. Appl. Phys. **71**, 4066 (1992).
[17] D. A. Hill, X. Huang, G. Bazán, and G. H. Bernstein, J. Appl. Phys. **72**, 4088 (1992).
[18] S. Mackie and S. P. Beaumont, Solid State Technol. 117 (1985).
[19] X. Huang and G. H. Bernstein (unpublished).
[20] T. H. P. Chang, J. Vac. Sci. Technol. **12**, 1271 (1975).
[21] J. S. Greeneich and T. van Duzer, IEEE Trans. Electron Device **ED-21**, 286 (1974).
[22] X. Huang, G. Bazán, D. A. Hill, and G. H. Bernstein, J. Electrochem. Soc. **139**, 2852 (1992).